STUDIES OF A GAS-FILLED ULTRAVIOLET DETECTOR WITH A SEMI-TRANSPARENT PHOTOCATHODE.

John Stuart Edmends* and David John Miller
Dept. of Physics and Astronomy
University College London
Gower Street, London WC1E 6BT, U.K

Fred Barlow
Instrument Technology Ltd
Castleham Road
Saint Leonards on Sea, East Sussex, U.K

ABSTRACT

A "pumpable tube" has been built in which a semi-transparent gold photocathode was exposed to ultraviolet light. It was filled with various pressures of methane, argon and neon, and configured as a triode, a tetrode or a pentode. Detailed results were obtained on photocathode and grid performance at different pressures and voltages. Used as an ultraviolet-sensitive photomultiplier it has reached an overall gas-gain of 9.5×10^4. This work is part of a programme to develop a gas-filled photomultiplier which will amplify scintillation pulses in the high magnetic fields of particle physics experiments at colliders.

* SERC CASE research student sponsored by Instrument Technology Ltd.

1. INTRODUCTION

Particle physics experiments require detectors which will detect Cerenkov or scintillation light inside regions of high magnetic field (typically 0.4 to 1.5 Telsa). For signals of less than a few hundred photons it is essential that there should be gain in the detector before even the best low-noise pre-amplifier can be used. The traditional technique has been to use photomultipliers with solid secondary-emission dynodes, but such photomultipliers will not operate in high fields. The work reported here confirms the suggestion (1,2) that a gas-filled tube with a semi transparent photocathode can achieve high gains (at least the 9.5×10^4 which was seen with this equipment). It is the first step of a development programme to produce gas-filled photomultiplier tubes.

Results are reported from work with a demountable tube-assembly configured as a parallel-plate diode, triode, tetrode or pentode. Diode data show variation of the quantum-efficiency of the photocathode with Ar, Ne and CH_4 fillings at pressures up to 100 torr, compared with vacuum. Triode and pentode data show the factors which effect transmission of photoelectrons and positive ions by a grid. Parallel-plate avalanche gain can be produced in the gas in all configurations. Results in the triode, tetrode and pentode configurations show that it is possible to use low fields to transfer electrons across the gap bordering the cathode and to produce large gains in the later stages without allowing many positive ions to return to the cathode. A large temporary increase in the sensitivity of the photocathode was

observed after it had been exposed to a continuous bombardment of positive ions.

This work with a demountable ultraviolet detector has been aimed at providing data for the manufacture of sealed tubes with cathodes sensitive to visible light, but the results could be of interest to those developing position-sensitive detectors for ultraviolet light. The parallel-plate amplification process is known to give good position resolution if suitable readout is provided (3). There may, in particular, be applications using barium fluoride scintillators (4) in positron emission tomography and related fields.

2. EQUIPMENT AND TECHNIQUES

2.1 Demountable Tube Assembly

The semi-transparent gold photocathode was deposited on a sapphire disc and mounted just inside a plane quartz window at the end of a cylinder of graded glass (figure 1). The other end of the cylinder was fused to a metal flange and clamped with a "CONFLAT" seal to a stainless steel plate with gas and electrical feedthroughs. The photocathode, grids and anode were carried on three parallel ceramic rods.

The tube was repeatedly opened and rearranged as the work progressed. That is why a gold photocathode was chosen which kept its small (5), but adequate, quantum-efficiency despite repeated exposure to atmosphere. The tube could be cleaned after closing by pumping to 5.10^{-6} Torr with a 3" diffusion pump, baking to 300°C and firing a getter (8). All gases were

of "research" grade, supplied in glass flasks. The glass connecting manifolds were also pumped at 10^{-6} Torr before filling. The pressure in the tube was measured with diaphragm gauges over the range from 10^{-3} to 100 Torr.

The electrode-carriers were stainless steel rings. Early results with ceramic carriers were unreliable because of the buildup of charge on the dielectric surfaces. By using conducting carriers such effects were completely dispelled. With a small light spot in the centre of the photocathode the electrons and ions stayed in the region of parallel field lines, well clear of the edges of the electrode-carriers. The anode was a flat disc of polished stainless steel.

Two kinds of grids were used. The "low density" grid was made from parallel 20 micron gold-plated tungsten-rhenium wires stretched at 1 mm spacing across the 20 mm circular gap in the electrode carriers. The "medium density" grid consisted of a square mesh of 80 μm diameter stainless steel wires with 1 mm spacing.

2.2 Light-Sources and Electronics

D.C. data were taken with an E.M.I. mercury vapour lamp with a quartz envelope. Currents from the electrodes were measured with a battery-powered pico-ammeter which could be switched into the different electrode-lines without disturbing the circuit.

A xenon flashlamp was used for pulsed operation (6). The pulse length was measured with a fast channel-plate detector

to be about 250 ns. Signals from the electrodes were displayed on an oscilloscope after integration with a charge pre-amplifier (7).

2.3 Interpretation of Pulses From Electrodes

When a charge moves towards or away from a solid electrode the rate of flow of current in the external lead is proportional to the rate at which the charge is moving through the electrostatic potential (see discussion in Appendix, following the work of Ramo (8)). Using the integrating pre-amplifier with its very long time constant it is possible to interpret the output voltage pulses on the oscilloscope directly in terms of integrated currents from the leads, ie. the charges arriving or passing through the electrodes. If the charge completely crosses the gap between two solid electrodes its full value is integrated with opposite signs on the two of them. If a compact cloud of charge passes through a grid and into the space beyond, the current in the leads to the grid is seen to reverse. A charge cloud can be regarded as "compact" if its length is much less than the length of the inter-electrode gaps in the tube. In the work reported here the electron clouds produced by the pulsed xenon lamp are not compact because the electron mobility is large; i.e. the pulse duration is longer that electron transit time across a gap. Thus we can measure the total charge of electrons only if they all are produced by or absorbed by the electrode whose pulse is being integrated. The positive ion cloud from avalanche gain can usually be treated as "compact" in this work because:-

a) Most of the gain occurs in the latter part of the gap (ie. gap size $\gg 1/\alpha$, where α is the first Townsend coefficient, see appendix) and

b) The positive ion transit time is much longer than the length of the xenon light pulse.

As discussed quantitatively in the appendix, when parallel-plate gas-gain occurs in a gap between two simple electrodes the pulses from both of them have similar characteristic shapes (with opposite polarity) consisting of a rapid voltage change followed by a slower, larger change in the same direction (see figure 2). The rapid signal is dominated by the electrons from the gain process which move quickly to the more positive electrode. Since most of them are produced close to this electrode they pass through only a small part of the inter-electrode potential so the rapid signal represents only a small part of the total charge of the electrons collected. The bulk of the positive ions must travel across most of the gap so they give a slower, larger signal.

3. RESULTS ON BASIC PROCESSES

3.1 The Effects Of Gases On Photocurrent

Figure 3 shows how the D.C. photocurrent varies with gas pressure, with various gas fillings, relative to vacuum, when the tube is set up as a simple photodiode. Note that methane gives the smallest effective reduction in quantum-efficiency, much better than the rare gases. These data were taken with a forward bias of 15 Volts. At higher voltages gas multipli-

cation can mask the effects of electron extraction from the photocathode.

After an initial reduction by about 35% at around 80 Torr. the quantum efficiency in methane levels off with increasing gas pressure. The currents in argon and neon are reduced by about 80% at 80 torr. and they continue to fall with increasing pressure. The effects of even higher pressures were not studied in detail because the voltages required to produce gain (see 4.1 below) become too high at pressures above a few tens of torr. The superior performance with polyatomic gases such as methane or isobutane was first suggested by Anderson et al (9), but variations of cathode efficiency meant that the effect was not completely clear. They also reported evidence that isobutane poisoned the photocathode.

3.2 Transmission Of Electrons Through Grids

With the tube set up as a triode, D.C. data were taken at low voltages to observe the effect of gases on the transmission of photoelectrons through the parallel wire "low density" grid (see 2.1 above). Figure 4 shows "Ramo plots" (see Appendix for full discussion) which illustrate how the calculated potentials in a parallel-plate triode behave with various voltages on the electrodes. The cusp around the grid wires is expected to cause some electrons to be collected by the grid even when a large positive voltage on the anode gives "field penetration" into the cathode-grid gap.

From figure 5 it can be seen that methane is much superior to argon in allowing electron transmission through the grid. In

fact, the transmission in methane is enhanced even compared with the same triode in vacuum. The cathode and the grid are both at ground potential. With more than 2 Torr. of methane in the tube an insignificant fraction of the photocathode current is lost to the grid as soon as a small positive voltage is placed on the anode -- i.e transmission is consistent with 100% when the field on the "output" side of the grid for electrons is greater than that on the "input" side ("Lo to Hi" conditions). No theoretical calculations have been made to explain this, but one may speculate that inelastic collisions with methane molecules "cool" the electrons so that they follow the local field lines, avoiding the grid wires which are more negative than the spaces between.

Pulsed data (figure 6) taken with 20 Torr. of methane in the pentode configuration show that the two densities of grid have very similar electron transmission characteristics when the field on the output side of the grid is less than that on the input side ("Hi to Lo" conditions). A magnified pulse was produced by gas-gain in the high-field region on the input side of either the second ("low density") or the third ("high density") grid, and the size of the incident electron cloud was measured from the sum of the rapid and the slower pulses (see discussion in 2.3 above) from the previous grid. The amount of this cloud transmitted through the grid was deduced from the size of the pulse from the subsequent electrode. This was grid 3 for the "low density" data or the anode for "medium density". The variable voltage on this next electrode

was always the highest positive voltage in the whole tube, so it collected all of the transmitted electrons.

Note that the data points on figure 6 lie on lines which do not go through the origin. This is to be expected. There are two separate effects at work. The low density grid allows field penetration from the input side to the output side. Adding this extra field to the applied output field is equivalent to moving the upper curve by about 130 V/cm to the right, which brings it on top of the curve for the medium density grid. The field penetration for the medium density grid itself is much smaller. But the transmission with the medium density grid, extrapolated back to zero applied field, is too high to be accounted for by field penetration. It is surely due to the inertia of fast electrons which miss the grid wires; a specifically low pressure effect.

3.3 Transmission Of Positive Ions Through Grids

Positive ions were produced in the grid-anode gap of the triode by raising the anode potential to give gas multiplication in D.C. conditions. Figure 7 shows the ratio of the positive ion cathode current to the sum of positive ion components of cathode and grid currents as a function of the applied field in the grid-anode gap for a wide range of gas pressures. All but one of the curves is for the "low density" grid. The upper limit of each curve represents the onset of sustained discharge breakdown in the second gap. The lower limit corresponds to such low gas-gain that subtraction of the initial photoelectron current becomes unreliable. Note that the minimum of ion transmission drops as gas pressure

rises to about 10 Torr., then levels off. The curve with the lowest ion return to the cathode is for the square meshed "medium density" grid.

A further comparison between the two types of grid was made in the pentode with the first and third grids of "medium density" and the second grid "low density" (see 3.2 above, discussion of figure 6). The pulsed xenon source was used and the voltages were arranged so that electrons transferred through the earlier gaps were multiplied with high gain in the later gaps, giving positive ions which moved back towards the photocathode. The positive ion components of the pulses were estimated by careful examination of the signals on the oscilloscope (see figure 2 and the discussion at 2.3 above). For the second ("low density") grid the transmission (figure 8) was deduced by comparing the pulse from that grid with the pulse from the first grid (with a low field between cathode and grid 1). For the first ("medium density") grid its slow pulse was compared with the slow pulse on the cathode.

There is a clear supression of positive ion transmission with the "medium density" grid, compared with the "low density" grid, both in the D.C. data (figure 7) and in the pulsed data (figure 8).

Ion transmission with the medium density grid is close to what would be expected from the theory of Buneman et al (10), which has been confirmed for electrons at atmospheric pressure by Schwarz et al (11). The transmission with the low density grid is about three times that expected if the ions were

simply following field lines, as suggested for electrons by Buneman et al and represented by the diagonal dashed line on figure 8. It is not clear how such large transmission comes about, but we conclude that for efficient shielding the grid density must be higher than some minimum
(e.g. $\rho > 0.2$ where $\rho = \frac{2\pi r}{d}$ is the parameter defined by Buneman et al, r is the wire radius and d the wire spacing for a parallel wire grid).

Figures 7 and 8 both refer to the situation where the "input" field at the grid for positive ions is greater than the "output" field ("Hi to Lo" for ions). It is hard to take clear data with the output field larger than the input field, since this gives larger gas multiplication on the high field side of the grid, but there are indications that the positive ion transmission is large in this configuration.

3.4 Ion Bombardment Of the Gold Photocathode

3.4(i) Variation of Sensitivity

It is known that photocathodes which are sensitive to visible light may loose their sensitivity after prolonged exposure to positive ions from gas multiplication (12). Such effects are indeed seen in the continuation of the present work with visible light-sensitive tubes (to be published shortly). This is not the case for the gold photocathode.

Two tests were made, with different amounts of positive ion charge delivered to the cathode.

a) The pentode was set up as an "effective triode" (V_k = -10, V_{g_1} = 0, V_{g_2} = 800, V_{g_3} = V_a = 0) with large gain in the second stage and modest positive ion transmission to the photocathode. The xenon flash lamp was run at 20Hz, giving a slow, delayed positive ion pulse of 0.3 picocoulombs per flash on the photocathode. After two hours (47 nanocoulombs on the photocathode) there was no change in the pulse-heights.

b) Gain was then also induced in the gap between the cathode and the first grid of the pentode (V_k = -600, V_{g_1} = 0, V_{g_2} = +750, V_{g_3} = V_a = 0). The positive ion charge delivered to the photocathode was initially 7.5 picocoulombs per pulse. After 20 hours at 28.6Hz the integrated positive ion charge which had arrived at the cathode was approximately 23 microcoulombs and the pulse-height had risen by a factor of 1.5. After 80 hours (approx. 110 microcoulombs) the pulse-height had doubled, and after 110 hours (170 microcoulombs) the pulses stabilised at approximately 2.8 times their initial size and did not change over a further 60 hours of running. The steady pulsing of the light was then stopped and short tests were made over a further period of days. The pulse-height slowly decreased until it returned to the original starting value.

We conclude from these tests that prolonged exposure to positive ion bombardment causes a significant temporary increase in the photosensitivity of the cathode.

4. STUDIES OF GAIN IN MULTI-STAGE TUBES

4.1 Overview And Definitions

Experiments were made to produce the largest possible overall gain in triode, tetrode and pentode configurations. In each case the voltage across the gap from cathode to grid 1 was kept small in order to reduce positive ion transmission through the grid to the cathode. Although secondary effects are not serious with the gold photocathode (see 3.4 above), such positive ion feedback causes both early breakdown and reduced cathode lifetime in tubes sensitive to visible light. The voltages on the other electrodes were varied to produce one or two stages of gas gain.

Two effects restricted the gain to less than might have been obtained with perfect planar grids and electrodes in a perfect tube:

a) The annular metal electrode carriers were thicker than the electrodes themselves, so at one side of a grid the gap would always break down at the voltage dictated by the carrier spacing, rather than what would have been expected from the grid spacing (see sketches in figures 4, 6, 9). This was the limiting mechanism at the highest gains.

b) The feedthroughs in the base of the tube began to break down to the grounded end plate at about 1 KV (depending on gas pressure). If the photocathode was set at a large negative voltage it was still possible to have two stages with over 600 volts potential difference in each. To achieve maximum gains

at higher gas pressures than about 20 torr. would have required higher voltages than the feedthroughs would allow.

The "effective gain" of the tube is defined as the size of the anode pulse from the preamplifier divided by the pulse which would be generated by the same length and intensity of flash when the tube is operated as an "effective diode", i.e. collecting the photoelectrons on the first grid at +20 volts, with the cathode and other electrodes at ground. It has two components, as explained in 2.3 above (see figure 2), both of which are of interest in particle-detector applications; the rapid component for for timing, and the slower for accurate pulse-height measurement. "Gain over vacuum diode" is the effective gain multiplied by a reduction factor (from figure 3) due to the effect of the gas on the photoemission efficiency of the cathode.

4.2 Triode Results With Methane And Argon

Figure 4 includes a sketch of the electrode spacings. Data were taken with the cathode and grid both grounded, relying on field penetration from the grid-anode space to transfer electrons from the grid. The pulsed gains before breakdown are shown in Table I.

The gain before breakdown with argon is much lower than with methane. The duration of each pulse in argon, at high gain, is much longer than at lower gain. The pulse duration in methane (see table I, column 4) is never more than a few microseconds. Both of these effects in argon are consistent with being due to secondary emission from conducting surfaces, caused either by the ultraviolet photons from excited argon

atoms in gas-multiplication showers or by the arrival of positive ions. Methane is known to screen out ultraviolet photons (13) and when methane ions hit a surface there is a higher probability for dissociation than for secondary electron emission.

The largest effective gain with the methane triode was x950 at 30 Torr. For fair comparison with other pressures this must be reduced to the "gain over vacuum diode" (Table I), so 2 Torr. seems as good as 30 Torr. and 11 Torr. is not much worse. More gain would have been obtainable in a "perfect" tube with ideal planar grids, since the breakdown was always between the electrode carriers.

4.3 Tetrode Results

The highest effective gain yet acheived was 9.5×10^4 at 11 Torr. (see figure 9). The two gain-stages were one after the other with an estimated gain of 43 in the gap between grid 1 and grid 2. [At 30 Torr it was not possible to get the voltage differences between the electrodes up to their breakdown values before the feedthroughs broke down.]

4.4 Pentode Results

The pentode was used with two gain-stages separated by a drift region. It worked well, but the highest gains were not achieved in the pentode because it required even higher overall voltages than the tetrode and was more severely limited by breakdown at the feedthroughs. The results in Table II show how the overall-gain (read from the grid pulses on the oscilloscope) varied with anode voltage. The trans-

mission of the positive ions through the grids could also be deduced from the pulses on the electrodes. For example, at maximum gain (last line on Table II) the positive ion return to the photocathode was estimated to be approximately 0.057% of the output anode pulse and 670% of the primary electron pulse from the cathode.

5. CONCLUSIONS

5.1 General

This work has clarified our understanding of the mechanisms that govern the performance of parallel-electrode multi-stage gas-filled phototubes. These results have already been utilised in the design, construction and operation of sealed tubes which are sensitive to visible light (to be published separately). Such sealed tubes cannot be reconfigured and refilled in the same way as the demountable rig used for the work described here, so a similar survey of gases, pressures and configurations with light-sensitive tubes would be much slower and prohibitively expensive.

Methane performs much better than argon or neon in three important respects:-

a) Methane inhibits photocathode emission less than the noble gases.

b) Methane allows more electrons to be transmitted through grids.

c) Breakdown comes at higher values of gas gain in methane.

Denser grids are more effective at stopping positive ions, though they make little difference to electron transmission.

It is possible to operate a gas filled tube like a multi-step proportional chamber (15), and to separate the gain stages from the photocathode, hence protecting it from heavy bombardment by positive ions.

5.2 For Ultraviolet Detectors

For possible applications to ultraviolet detectors, it is interesting that in none of this work were any signs seen with the gold photocathode of the two most serious problems that exist with the more efficient visible light-sensitive photocathodes:

a) Positive ion bombardment caused a temporary increase in quantum efficiency, rather than a decrease as has been reported for light-sensitive cathodes.

b) There was no evidence of significant secondary emission of electrons from the gold photocathode when hit by positive ions. (Clear delayed pulses have been seen with light-sensitive photocathodes).

This suggests that it may be possible to run a methane-filled detector with a high forward field on the gold photocathode, enhancing electron emission and giving immediate first-stage gain. Large gains before breakdown might even be obtained in diode mode, with a significant fast component for timing

purposes. This could be of interest to those attempting to develop Barium Fluoride position-sensitive detectors for positron annihilation photons.

APPENDIX

Pulse Formation due to Moving Charges and Avalanches

A1. Point Change in General Electrode Structure

Following Ramo (8), the instantaneous current flowing to any electrode E in a "tube" (be it drift chamber, phototube, radio valve etc) due to charge q at point r, moving with velocity v(r) in the space of the tube, is

$$i_E = -q \; \underline{E}_E(\underline{r}).\underline{v}(\underline{r}) \qquad (A.1)$$

where $\underline{E}_E(\underline{r})$ is the "Ramo field", the electric field which would be produced at the position of the charge in the following circumstances:-

i) charge q removed;

ii) electrode E raised to unit potential;

iii) all other electrodes held at zero potential;

In the simple example of a plane parallel diode with solid anode at $z = z_a$ and solid cathode at $z = 0$, (A.1) becomes, for the anode current

$$i_a = -q \; \frac{1}{z_a} \; \frac{dz}{dt} \qquad (A.2)$$

and, for the cathode current,

$$i_k = +q \; \frac{1}{z_a} \; \frac{dz}{dt} \qquad (A.3)$$

since $\underline{E}_E .v$ reverses in sign when unit potential is placed on the cathode instead of on the anode. When charge q moves a distance $\Delta \underline{r}$ in time Δt in the general case, the net charge flowing to electrode E will be

$$\Delta q_E = -q \int_t^{t+\Delta t} \underline{E}_E.\underline{v} \; dt \qquad (A.4)$$

If we write $\underline{E}_E = -\underline{\nabla} V_E$, where V_E is the associated "Ramo potential"; and $\underline{v} = d\underline{r}/dt$

then

$$\Delta q_\epsilon = +q \int_{r}^{r+\Delta r} (\nabla V_\epsilon).dr = q \Delta V_\epsilon \qquad (A.5)$$

That is, the charge flowing to electrode E due to the point charge moving through distance r is proportional to the change ΔV_ϵ over the path Δr. Returning to the simple example of the plane parallel diode, $E_\epsilon = -\nabla V_\epsilon = -\frac{1}{z_a}$ for the anode, and the motion of all charges is taken to be along the + z direction, hence the charge flowing to the anode is

$$\Delta q_a (\Delta z) = q \frac{\Delta z}{z_a} \qquad (A.6)$$

Or, if q crosses the whole gap from cathode to anode, $\Delta z = za$ and

$$\Delta q_a = q$$

$$(= -\Delta q_k, \text{ c.f (A.3)})$$

A2. Plane Parallel Triode

For a tube with more complicated geometry, electrodes may screen one another and motions are not necessarily along the direction of E for the electrode of interest. Figure 4 shows, as a simple example, two "Ramo plots" for a plane parallel triode with unit potential placed, in turn, on the wire grid and on the anode. The alternative curves in the region of the grid represent paths which pass either through a wire or through the middle of the gap between wires. Note

i) for unit potential on the anode, the grid-cathode space is not fully screened. A charge moving there causes current to flow from the anode proportional to E_a, the "Ramo field" due to the anode which is represented by the slope of the plot, and

ii) a point charge which passes through the grid does not rise to the full unit potential in the region of the grid, so (by A.5) its approach does not induce as large an integrated pulse on the grid as a charge which is captured. After the charge has passed through the

grid there will be a reversed current to the grid as the charge moves away in the reversed "Ramo field".

A3. Charge Distributions in Avalanches

In the work presented above two simplification can be made to the description of a Townsend avalanche

a) Electrodes are always parallel and flat.

b) The duration of the light pulse is long compared with the transit time of electrons across any gap.

The latter point means that the shape of any charge pulse due to electrons arriving at an electrode is dictated by the length of the light pulse, whereas the shapes of pulses due to positive ions (with mobility $\sim 10^{-3}$ that of electrons) are largely governed by the motion of ions.

If one electron initiates an avalanche in a gap from z = 0 to z = z then the shower at depth z will contain N(z) electrons, on average, where

$$N(z) = \exp(\alpha z) \qquad (A.7)$$

and α is the first Townsend coefficient.

Apart from the initiating electron, each electron in the shower is associated with a positive ion which - assuming no recombination - will return slowly to the negative electrode.

The distribution of numbers of ions produced in the gap is

$$\frac{dN}{dz} = \alpha \exp(\alpha z) \qquad (A.8)$$

This is, of course, the distribution of starting points for both secondary electrons and positive ions, both of which cause induced

currents to flow to the electrodes as they move through the gap. Because of the exponential growth of the avalanche, most ionisation takes place close to the more positive electrode of a gap and the electrons move through only a small part of gap width, producing integrated charge pulses on the electrodes which are only a small fraction of the actual charge of the electrons. Most positive ions, however, cross almost the whole gap so their integrated charge pulses add up to almost their whole charge.

For a simple plane parallel diode, the integrated charge pulse on the anode due to electrons (primary and secondary) from an initial pulse Q starting at z = 0 is obtained by integrating (A.6), with $\Delta z = (z_a - z)$ and with the secondary charge weighted by $\frac{dN}{dZ}$ from (A.8),

$$\text{is } Q_e = Q_o \{1 + \int_0^{z_a} \frac{(z_a - z)}{z_a} \alpha \exp(\alpha z)\, dz\} \qquad (A.9)$$

and the contribution due to the positive ions returning to the cathode is

$$Q_i = -Q_o \int_0^{z_a} \{-\frac{z}{z_a} \alpha \exp(\alpha z)\, dz\} \qquad (A.10)$$

where the two minus signs come from the opposite sign of the charge and from the opposite slopes of the "Ramo fields" for anode and cathode; $\underline{E}_a = -\underline{E}_k$. Thus the net induced charge signal on the anode due to electrons plus ions is just

$$Q_e + Q_i = Q_o \{1 + \int_0^{z_a} \alpha \exp(\alpha z)\, dz\}$$

$$Q_{TOTAL} = Q \{1 + \exp(\alpha z_a)\} \qquad (A.11)$$

(i.e. the total charge of the secondary electrons)

There is an equal and opposite induced charge on the cathode.

The first rapid contribution due to electron motion is

$$Q_e = Q_o [1 + \{\exp(\alpha z) - \int_0^{z_a} \frac{z}{z_a} \alpha \exp(\alpha z)\, dz\}] \qquad (A.12)$$

while the slower component due to the ions is

$$Q_i = Q_o \int_0^{z_a} \frac{z}{z_a} \alpha \exp(\alpha z)\, dz \qquad (A.13)$$

Integrating by parts,

$$Q_i = Q_o \{\exp(\alpha z_a) - \frac{\exp(\alpha z_a)}{\alpha z_a} + \frac{1}{\alpha z_a}\} \qquad (A.14)$$

and $$Q_e = Q_o [1 + \frac{1}{\alpha z} \{\exp(\alpha z_a) - 1\}] \qquad (A.15)$$

$$\simeq \frac{Q_{total}}{\alpha z} \quad \text{if } \exp(\alpha z) \gg 1 \qquad (A.15a)$$

Thus, at high gas gain, the rapid electron pulse is - as expected - only a fraction of the total pulse (figure 2). (This effect is more marked in proportional wire chambers where the gain occurs within a few tens of microns of the anode, limiting the distance travelled by secondary electrons even more than in the parallel plate case).

Table I

Methane Filled Triodes

Methane Pressure	Maximum Effective Gain	Maximum Gain Over Vacuum Diode	Pulse Duration at Maximum Gain (μs)
0.4	100	95	1
2	730	645	1.25
11	650	508	3
30	950	684	4

Argon Filled Triodes

Argon Pressure	Maximum Effective Gain	Maximum Gain Over Vacuum Diode	Pulse Duration at Maximum Gain (μs)
0.4	34	27	40
2	100	52	40
11	22.5	8	35

Table II

20 Torr Methane Pentode
Data on the 20 Torr methane pentode with two stage gas gain $g_1 \longrightarrow g_2$ and $g_3 \longrightarrow$ anode. The $g_1 \longrightarrow g_2$ gain was 143 ± 5.

$V_a - V_{g3}$	Effective two-stage Gain	Gain over Vacuum Diode
400	60 ± 5	43 ± 3
500	156 ± 10	112 ± 7
600	850 ± 20	612 ± 14
650	1900 ± 200	1368 ± 144
700	4200 ± 300	3030 ± 200
750	12000 ± 1000	8600 ± 700
800	Breakdown at feedthrough	

REFERENCES

1. C. Gallet, G. Nixon, D.J. Miller, P. Sanford; University College London internal note; 29 January 1982.

2. F. Sauli; CERN - EP/82-26 and Nuclear Instruments and Methods, 203, (1982) 601.

3. H. Schwarz and I.M. Mason; Nature 309, (1984) 532.

4. See e.g. Review by G. Charpak (CERN) at 1986 Vienna Wire Chamber Meeting, proceedings to be published in Nuclear Instruments and Methods.

5. A. Hughes and L. Dubridge; "Photoelectric Phenomena", McGraw Hill, N.Y. 1932.

6. E.G. & G. Electro-Optics bulb type FX108B-UV.

7. Canberra type 2003.

8. S. Ramo; Proceedings of Inst. of Radio Eng., Sept 1939, p584.

9. D.F. Anderson, R. Bouchier, G. Charpak, S. Majewski and G. Kneller; Nucl. Instr. and Meth. 217 (1983) 217.

10. O. Bunneman, T.E. Cranshaw and J.A. Harvey; Can. J. Res. 27 (1949) 191.

11. H.E. Schwarz, J. Thornton and I.M. Mason; Nucl. Instr. and Meth. 225 (1984) 325.

12. G. Charpak, W. Dominick, F. Sauli, S. Majewski; I.E.E.E. Trans. Nucl. Sci.; NS30, (1983) 134.
Positive ions also cause reductions in the cathode sensitivity of microchannel plate multipliers; see e.g. Hamamatsu TV Co Ltd, Technical Manual RES 0795.

13. M. Rose and S. Korff; Phys Rev 59 (1941) 850. See also F. Sauli "Principles of Operation of Multiwire Proportional and Drift Chambers"; CERN 77-09 (pp39 and 47).

14. S. Korff and H. Kallmann, "Electron and Nuclear Counters", Van Nostrand (1946).

15. F. Sauli; Physica Scripta 23 (1981) 526.

Fig 1

The Demountable Tube Assembly

Fig 2

Pulse due to Gas Gain in a Single Gap

The upper trace shows the characteristic sharp rise (less than one scale division) from electrons which go directly to the +ve electrode, followed by a slower rise as +ve ions cross the gap (the charge preamplifier integrates and inverts). The lower trace is from an unamplified silicon photodiode which monitors the flash of the xenon lamp. Scale 1 volt per division, 1 μ sec per division.

Fig 3

Effect of Gases on Photo current

Tetrode set up as effective photodiode ($V_{CATHODE}$ = -15 Volts. $V_{GRID_1} = V_{GRID_2} = V_{ANODE} = 0$). DC operation.

Fig 4

"Ramo Plots" of Calculated Potentials in Triode

See appendix for discussion of Ramo's method (8) for calculation of pulses on electrodes. Curves show the potentials along two lines; the first passing between grid wires; the second passing through a grid wire (with cusp).

a) V_A = 1 Volt; $V_k = V_G = 0$

b) V_G = 1 Volt; $V_A = V_k = 0$

[The third case (V_k = 1 Volt, $V_A = V_G = 0$) is similar to a) but reflected about the grid position].

Fig 5

Transmission of Photoelectrons by Grid; Effect of Gases

$V_k = V_G = 0$ in Triode; so "applied" field in grid-cathode gap ["input side" for electrons] is smaller than "applied" field in grid-anode gap ["output side" for electrons] (i.e. "Lo to Hi" conditions). The "applied" field, here and for subsequent figures, is calculated by simply dividing the potential difference across a gap by the gap spacing; i.e. no allowance for field penetration.

Fig 6

Transmission of Electrons in "Hi to Lo" Conditions

20 Torr of methane in pentode. See text for how different grids were selected. "Applied" field at "input side" of grid was set up in each case to be 1725 volts/cm. The dashed line represents the ratio of the "applied" output to input fields.

Fig 7

Transmission of Positive Ions by Grids: D.C.

Triode data. Positive ion current to cathode divided by sum of positive ion currents to grid and cathode (photoelectron current subtracted).

All the curves except the one marked "medium density" are for the low density grid (parallel 20 μm wires at 1 mm spacing. Note that the medium density grid (80 μm wire with 1 mm squares) gives the highest ion collection, i.e. the smallest rate of ion return to the photocathode.

Fig 8

Transmission of Positive Ions by Grids: Pulsed

Pentode; 20 Torr of methane. Note that the denser grid gives much reduced transmission. "Applied" field at the input side of the grids (for positives) was 1250 Volts/cm (i.e. "Hi to Lo" conditions). The dashed line represents the ratio of the "applied" input to output fields. See figure 6 for dimensions and electrode-labelling.

Fig 9

Tetrode Gain at 11 Torr

V_K = - 600, V_{G1} = - 590, V_{G2} = 0, V_A variable.

Two gain stages in succession; G1 to G2 and G2 to A.

Fig 1 The Demountable Tube Assembly

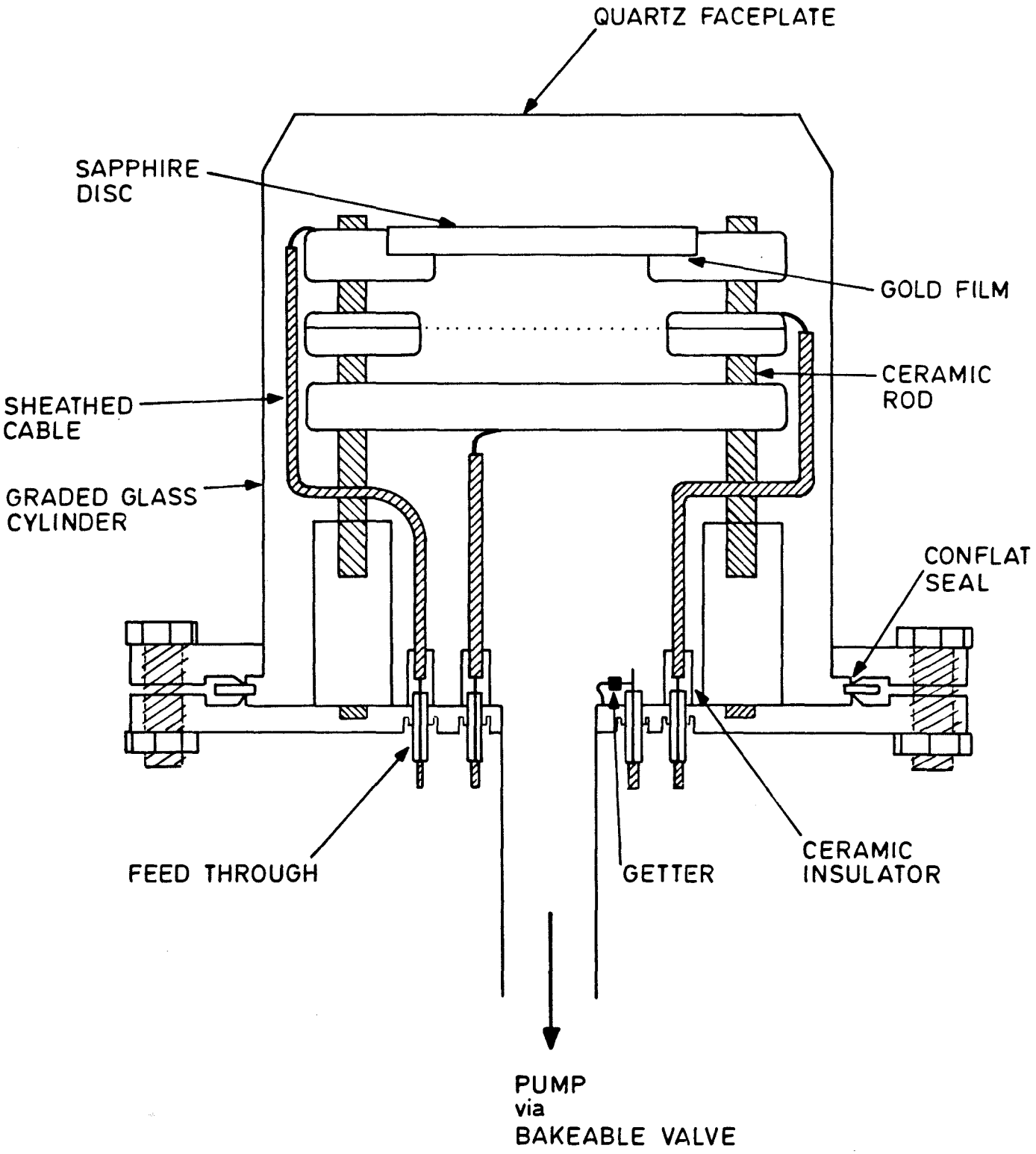

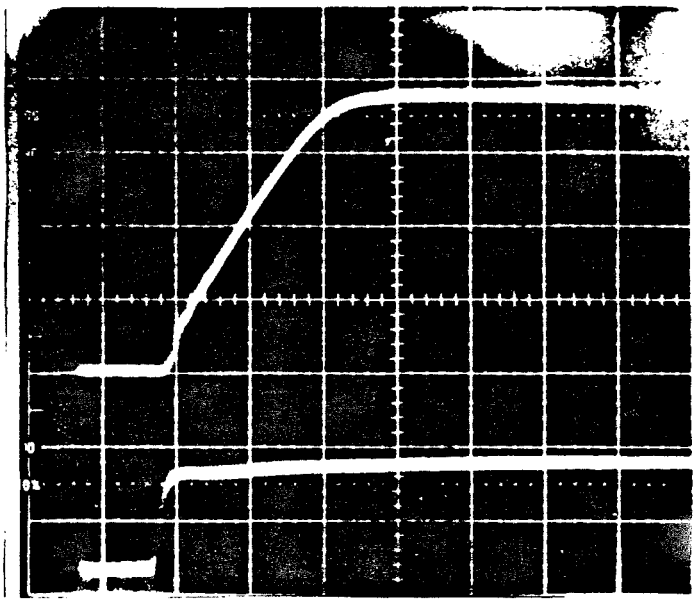

Fig 2 Pulse due to Gas Gain in a Single Gap

Fig 3 Effect of Gases on Photo current

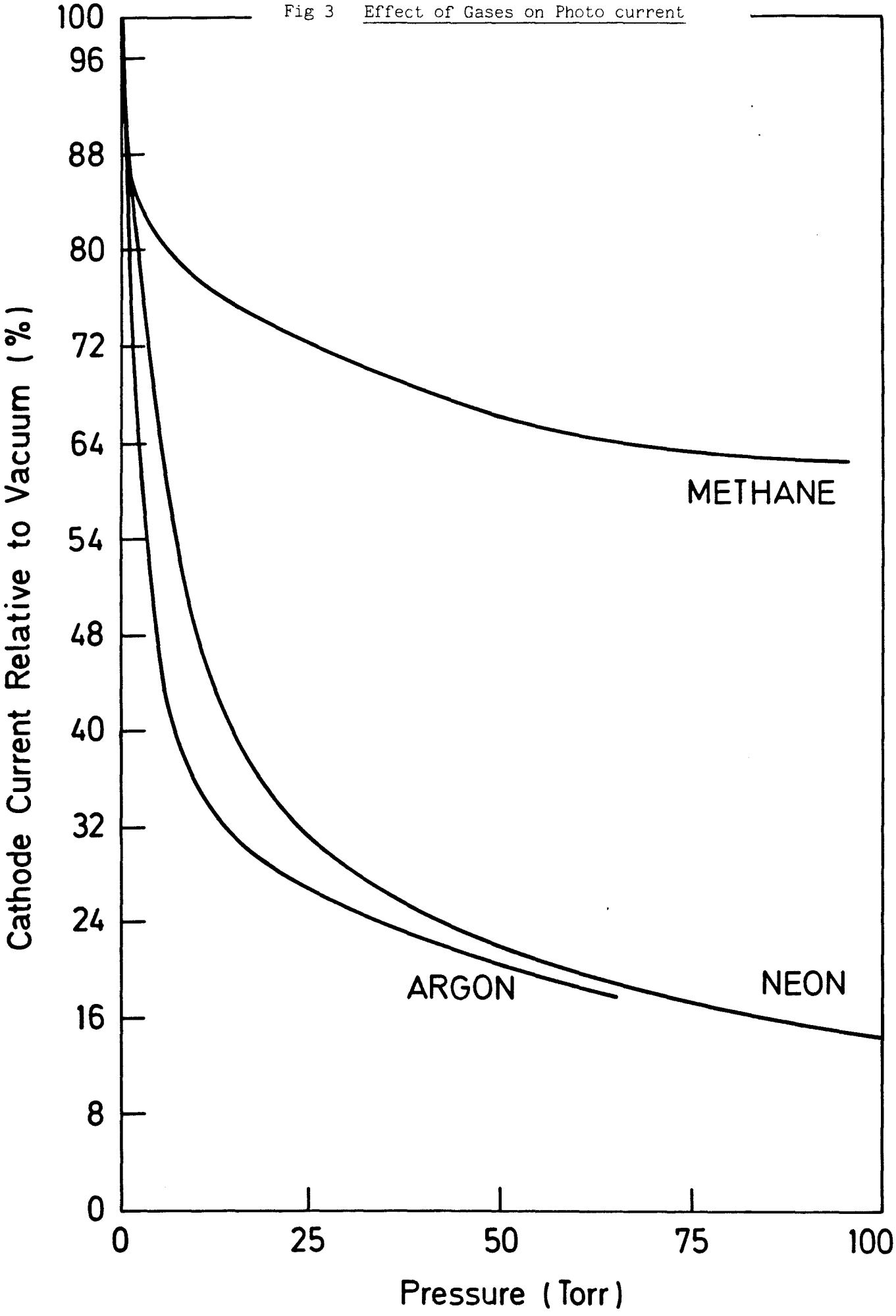

Fig 4 "Ramo Plots" of Calculated Potentials in Triode

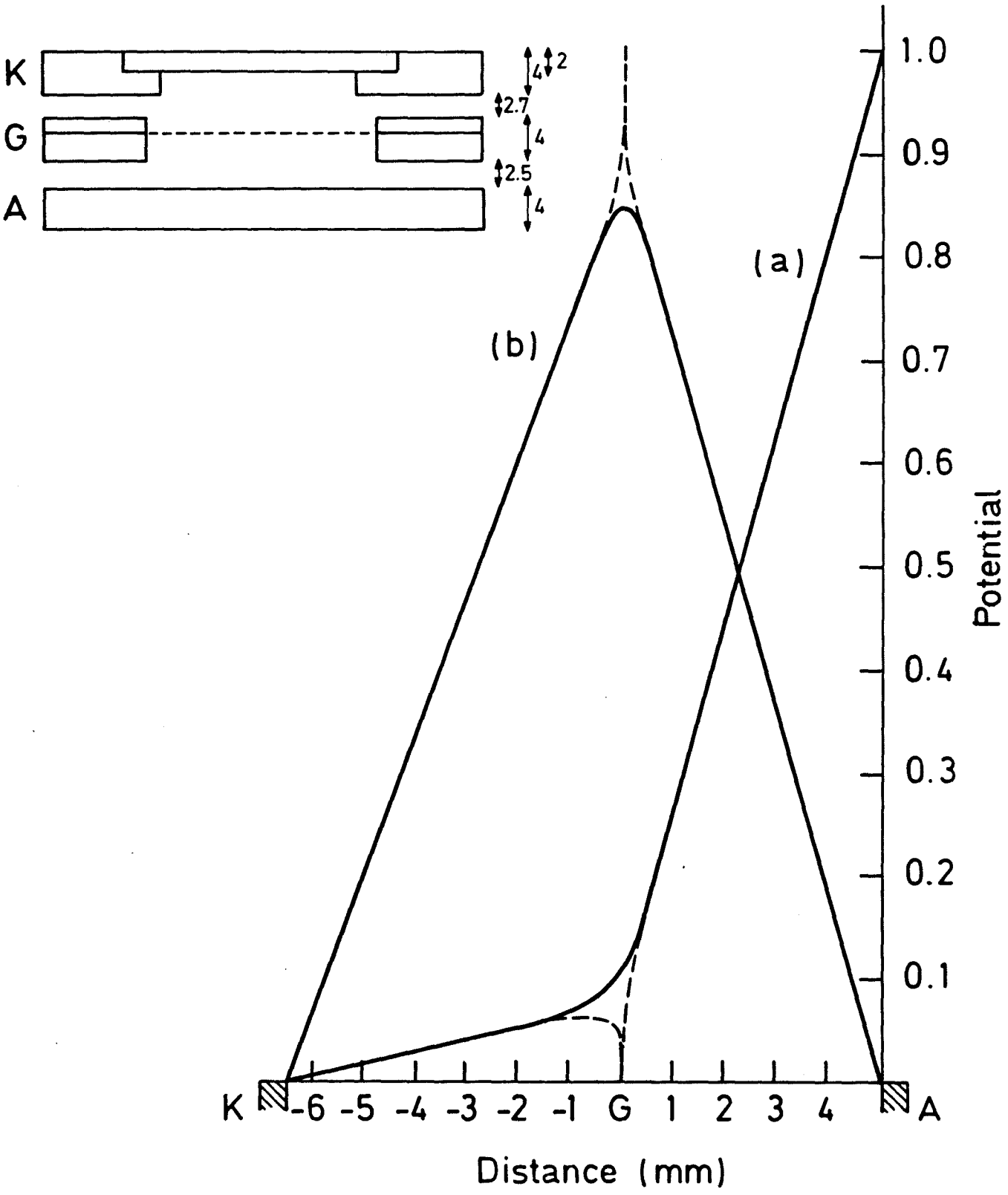

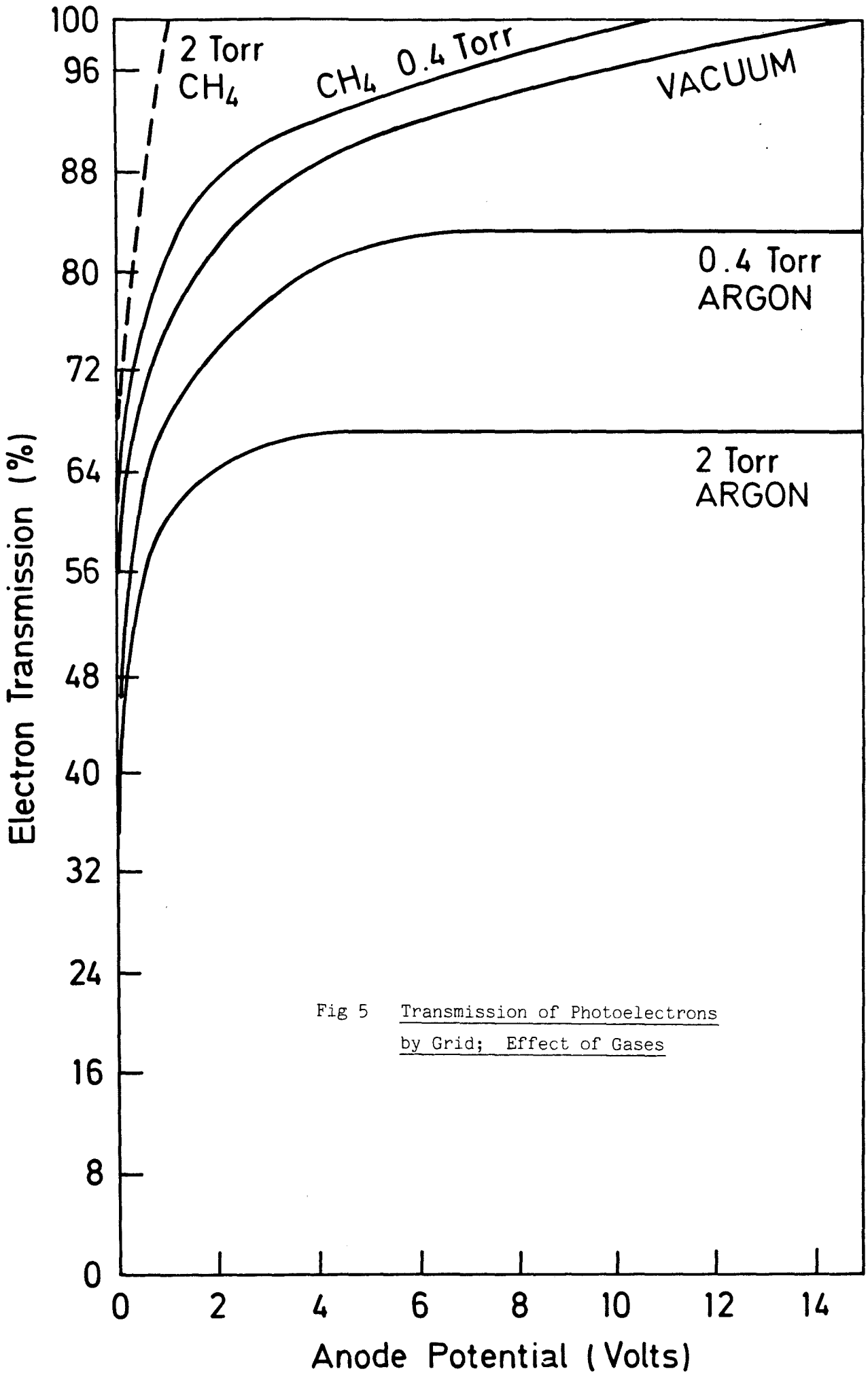

Fig 5 Transmission of Photoelectrons by Grid; Effect of Gases

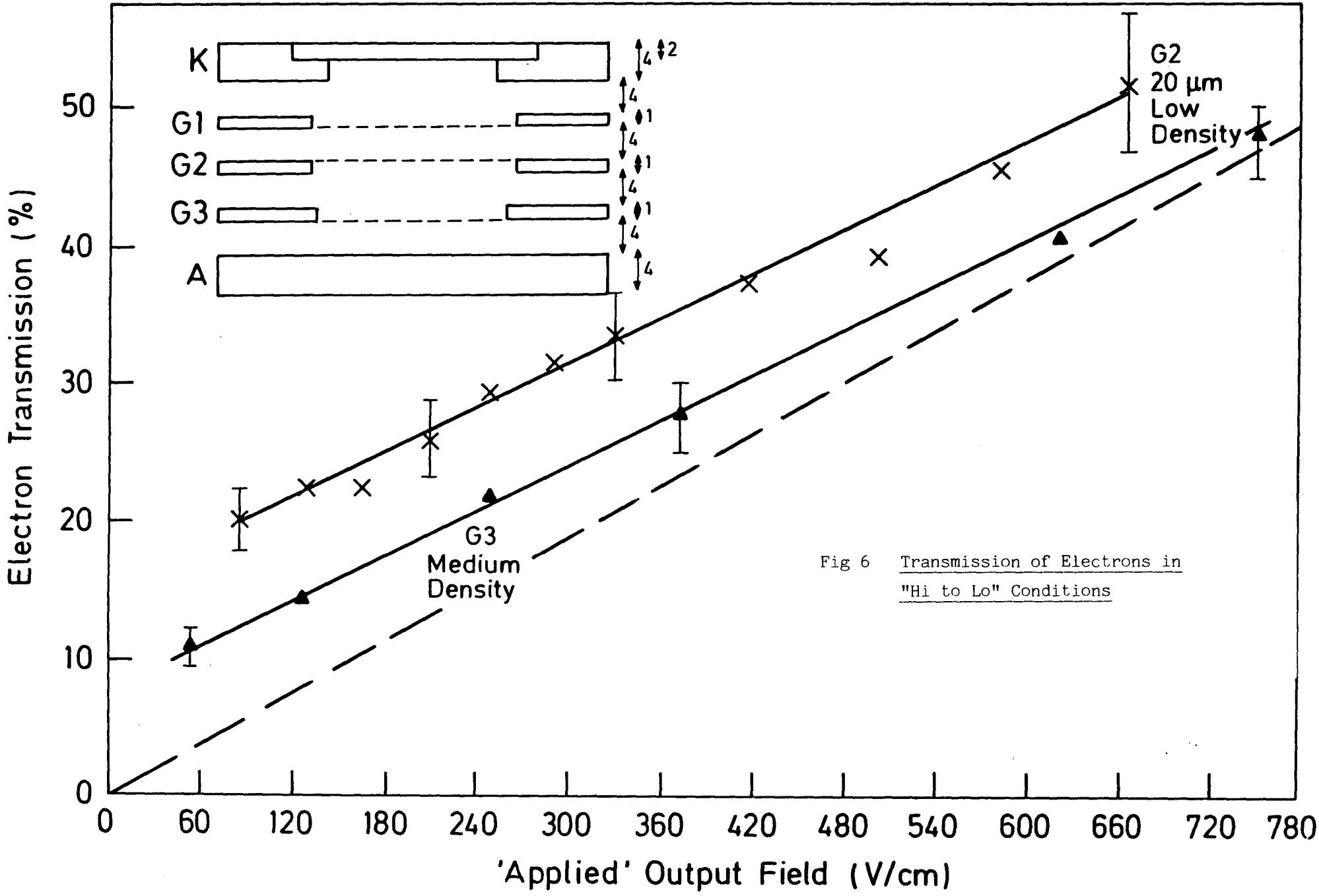

Fig 6 Transmission of Electrons in "Hi to Lo" Conditions

Fig 7 Transmission of Positive Ions by Grids; D.C.

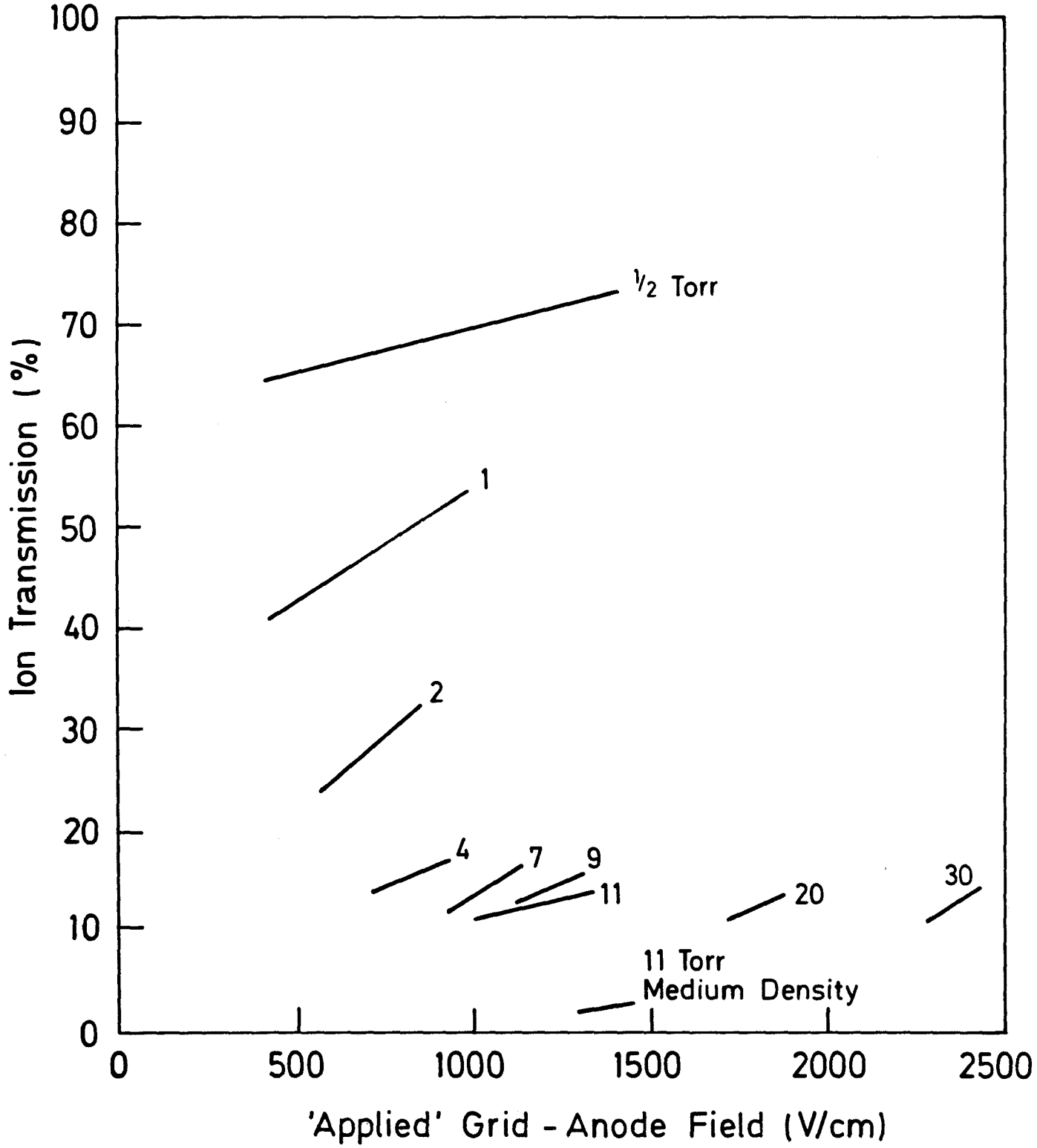

Fig 8 Transmission of Positive Ions by Grids; Pulsed

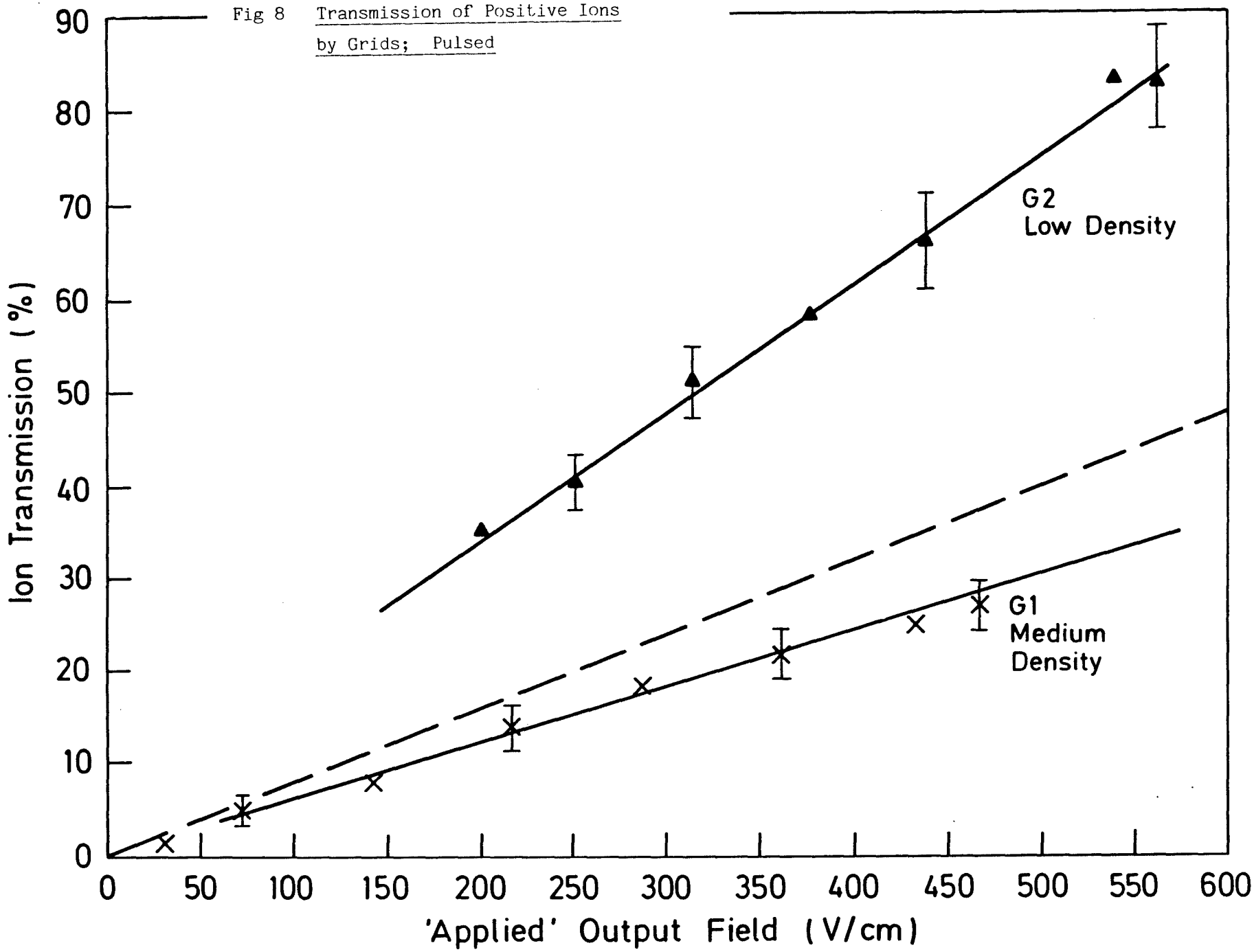

Fig 9 Tetrode Gain at 11 Torr